EPJ Web of Conferences **271**, 08006 (2022) https://doi.org/10.1051/epjconf/202227108006
HYP2022

Directed flow of Λ from heavy-ion collisions and hyperon puzzle of neutron stars

Akira Ohnishi[1,*], *Asanosuke* Jinno[2], *Koichi* Murase[1], and *Yasushi* Nara[3]

[1]Yukawa Institute for Theoretical Physics, Kyoto University, Kyoto 606-8502, Japan
[2]Department of Physics, Faculty of Science, Kyoto University, Kyoto 606-8502, Japan
[3]Akita International University, Yuwa, Akita-city 010-1292, Japan

Abstract. We examine the Λ potential from the chiral effective field theory (χEFT) via the Λ directed flow from heavy-ion collisions. We implement the Λ potential obtained from the χEFT in a vector potential version of relativistic quantum molecular dynamics. We find that the Λ potentials obtained from the χEFT assuming weak momentum dependence reproduce the Λ directed flow measured by the STAR collaboration in the Beam Energy Scan program. While the Λ directed flow is not very sensitive to the density dependence of the potential, the directed flow at large rapidities is susceptible to the momentum dependence. Thus understanding the directed flow of hyperons in a wide range of beam energy and rapidity is helpful in understanding hyperon potentials in dense matter.

1 Introduction

The hyperon puzzle is one of the central issues in neutron star physics in view of hypernuclear and strange particle physics [1]. When empirical two-body interactions are considered, hyperons are predicted to appear in the neutron star matter at (2-4)ρ_0, soften the dense nuclear matter equation of state (EoS), and reduce the maximum mass of neutron stars to be $M_{\rm max}$ = (1.3-1.6)$M_\odot$. Since several neutron stars are found to have masses around $2M_\odot$ or more, most of the proposed hyperonic matter EoS were ruled out. Thus something is wrong, and it is a challenge to elucidate the mechanism to solve this hyperon puzzle.

Among several solution candidates to the hyperon puzzle, we here concentrate on the solution based on the three-body YNN repulsion [2]. Since the three-body NNN interactions are known to be necessary to describe $A = 3$ nuclear binding energies and saturation point of nuclear matter, it is natural to expect that the three-body YNN interactions play some role in hypernuclei and hyperonic matter. However, there is almost no information on three-body YNN interactions from experiments, and we have to rely on theoretical predictions. For example, the chiral effective field theory (χEFT) is a first-principles framework and is expected to give reliable results once the relevant low-energy constants are determined. There are several predictions of the Λ potential $U_\Lambda(\rho)$ at high densities obtained by using χEFT [3, 4]. In Ref. [3], Gerstung, Kaiser, and Weise (GKW) calculated U_Λ in neutron star matter using χEFT under the assumption that the diagrams relevant to the three-body forces are saturated by the decuplet baryon propagation [5]. The obtained U_Λ with 2+3-body interactions is more

*e-mail: ohnishi@yukawa.kyoto-u.ac.jp

repulsive at high densities than that only with 2-body interactions, and it suppresses Λ to appear in neutron stars: the single particle energy of Λ at zero momentum is larger than the neutron chemical potential, $M_\Lambda + U_\Lambda(\rho, \boldsymbol{p} = 0) > \mu_n(\rho)$. Confirmation of the repulsive U_Λ at high densities is a challenge in hypernuclear and strangeness particle physics. Actually, one of the main goals of the J-PARC hadron hall extension [6] is to extract the three-body YNN interaction via precision experiment of hypernuclear spectroscopy.

Together with the hypernuclear spectroscopy, hyperon observables from heavy-ion collisions should be useful, since the formed nuclear matter reaches high densities. Specifically, the anisotropic flows such as the directed flow, $v_1 = \langle \cos\phi \rangle$ with ϕ being the azimuthal angle relative to the reaction plane, are generated in the initial stage and have been utilized to constrain the equation of state (EoS). Recently, the directed flow slopes (dv_1/dy) for identified hadrons were measured in the colliding energy range of 3 GeV $\leq \sqrt{s_{NN}} \leq$ 200 GeV [7]. The transition of the slope from positive to negative was discovered for both protons and Λs at $\sqrt{s_{NN}} \approx 10$ GeV. Theoretical models with a first-order phase transition predict this transition point at much lower beam energies [8], and the transition occurs at higher beam energies in hadron transport models without potential effects [9]. Recently, the proton directed-flow in the above colliding energy range was explained by a transport model [10] with a purely hadronic EoS. A repulsive EoS contributes positively to the slope in the early compression stage, while the tilted ellipsoid of the formed matter causes a negative contribution in the late expansion stage. With increasing colliding energy, the negative contribution takes over the positive one, and then the above transition of the slope is realized. The nuclear mean field including both the density and momentum dependence explains the observed transition energy [10].

Thus, we expect that the Λ directed flow is sensitive to the Λ potential at high densities. Provided that the above-mentioned compression/expansion mechanism also applies to Λ, one expects that the directed flow of Λs should be small since Λs are produced during the compression stage and the positive contribution would be smaller. Then the agreement of the transition energies of protons and Λs may suggest more repulsive potential for Λs than for protons at higher densities, as suggested by the χEFT.

In the Hyp2022 presentation, we discussed the effects of Λ potential on the directed flow of Λ by using an event generator JAM [10, 11]. The density and momentum dependences of the Λ potential are taken from the χEFT in Refs. [3] and [4], respectively, as discussed in Sec. 2. In Sec. 3, we discuss the results of transport model calculations using JAM performed in the relativistic quantum molecular dynamics mode with a Lorentz-vector implementation of the potential (RQMDv) [10]. Readers are referred to Ref. [12] for the details of the transport model and the calculated results.

2 Λ potential from chiral effective field theory

The Λ potential as a function of baryon density has been studied extensively in Refs. [13, 14], where the Λ separation energies of various hypernuclei have been well fitted and the EoS of the neutron-star matter has been predicted. However, most of them fail to sustain massive neutron stars [1]. While it is possible to increase the maximum mass of neutron stars above 2 $M_\odot$ by introducing repulsive three-body YNN interactions or repulsive hyperon potentials at high densities [2], most of these prescriptions introduce additional parameters which are not constrained by data or first principles.

A promising way to systematically describe many-body interactions is to invoke the χEFT, which is a first-principles theory based on the chiral symmetry of QCD. As shown in the left panel of Fig. 1, the Λ potential in nuclear matter was computed by GKW [3]. In uniform nuclear matter, the Λ potential is given as a function of the density and momentum,

$U_\Lambda(\rho, \boldsymbol{p})$. As shown in the right panel of Fig. 1, the momentum dependence of U_Λ in the χEFT is given, for example, by Kohno [4]. By including the three-body YNN interaction, the Λ potential becomes more repulsive at high densities and momenta.

We have parameterized the density and momentum dependence of the single-particle Λ potential U_Λ from χEFT in the Lorentz-vector type potential [15],

$$U^\mu_\Lambda(\rho, \boldsymbol{p}) = \frac{J^\mu}{\rho} U_{\rho\Lambda}(\rho) + U^\mu_{m\Lambda}(\rho, \boldsymbol{p}), \tag{1}$$

$$U_{\rho\Lambda}(\rho) = au + bu^{4/3} + cu^{5/3}, \tag{2}$$

$$U^\mu_{m\Lambda}(\rho, \boldsymbol{p}) = \frac{C}{\rho_0} \int d^3p' \frac{p^{*\prime\mu}}{p^{*\prime 0}} \frac{f(x, p')}{1 + [(\boldsymbol{p} - \boldsymbol{p}')/\mu]^2}, \tag{3}$$

where J^μ is the baryon current, $u = \rho/\rho_0$ is the nucleon density normalized by the saturation density $\rho_0 = 0.168$ fm^{-3}, and $p^{*\mu} = p^\mu - U^\mu$ and $p^{*0} = \sqrt{m_N^2 + \boldsymbol{p}^{*2}}$.

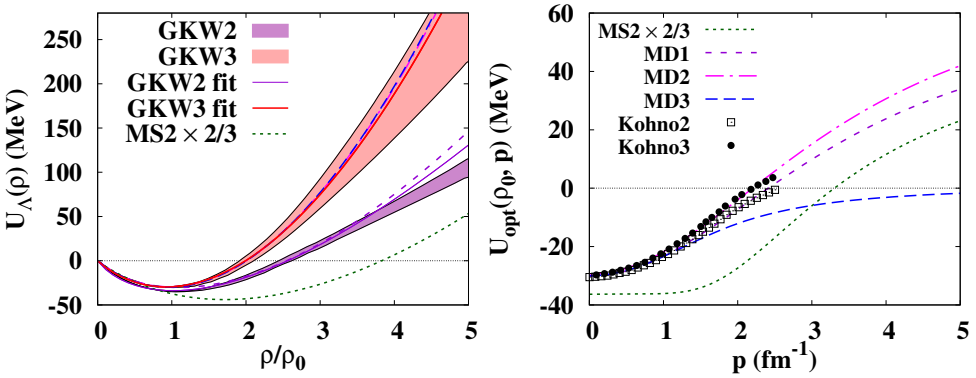

Figure 1. Baryon-density (left) and momentum (right) dependence of the single-particle potentials for Λ. GKW2 and GKW3 represent the Λ single-particle potential from χEFT with 2- and 2+3-body interactions [3]. MS2×2/3 shows the nucleon single-particle potential multiplied by 2/3. MD1, MD2, and MD3 are momentum-dependent potentials obtained by fitting the χEFT results [4].

In Fig. 1, we show the fitting results of the Λ potential. MD1 and MD2 potentials (right panel) are obtained by fitting the χEFT results by Kohno [4] at $\rho = \rho_0$ with 2- and 2+3-body interactions, respectively, up to the momentum of 2.5 fm^{-1} $\simeq \lambda$ (cutoff) assuming the range parameter $\mu = 3.23$ fm^{-1} [10]. The real part of the optical potential $U_{\rm opt}$ is defined as the difference between the single-particle energy and the kinetic energy. Since the momentum dependence in Ref. [4] seems to be stronger than the previous estimate [16], the potential with a weaker momentum dependence (MD3) is also prepared. For MD3, we require that the optical potential is zero at high momentum ($p \simeq 8.6$ fm^{-1}) and reproduces the result of Ref. [4] at $p = 1$ fm^{-1} $\simeq 0.4\,\lambda$. The density dependence (left panel) is determined by fitting the χEFT results by GKW [3]. GKW2 and GKW3 potentials are those with 2- and 2+3-body interactions, respectively. Since the Brückner-Hartree-Fock calculation was found to be unstable at $\rho/\rho_0 > 3.5$ [3], we fit the χEFT results in the range $\rho/\rho_0 \le 3$. At zero Λ momentum in cold nuclear matter, we find $J^\mu = (\rho, \boldsymbol{0})$ and $\boldsymbol{U}_{m\Lambda} = \boldsymbol{0}$, and thus $U_\Lambda(\rho) \equiv U^0_\Lambda(\rho, \boldsymbol{0}) = U_{\rho\Lambda}(\rho) + U^0_{m\Lambda}(\rho, \boldsymbol{0})$. The density dependence from the momentum-dependent interaction (second term) can be absorbed by tuning parameters (a, b, c), so the density dependence of U_Λ is almost the same with and without the momentum-dependent

potentials: GKW2 fit (thin solid, without momentum dependent terms) and GKW2+MD1 (dashed), and GKW3 fit (thick solid) and GKW3+MD2/MD3 (dash-dotted, long dashed) at $\rho/\rho_0 \leq 3$.

3 Directed flow of Λ from heavy-ion collisions

In order to simulate high-energy heavy-ion collisions, we use an event generator JAM2.1 [17]. In JAM2.1, there are several updates: one can utilize Pythia 8 [18] library as it is, potentials for leading baryons are included during their formation time with the reduced factor, and collision time and ordering time has been modified [19].

We implement the Λ potential described in the previous section in the form of Lorentz-vector potential in the relativistic quantum molecular dynamics (RQMDv) approach [10]. The RQMDv equations of motion for the i-th particle having the position q_i^μ and the momentum p_i^μ is given by [20]

$$\frac{dq_i^\mu}{dt} = v_i^{*\mu} - \sum_j v_j^{*\nu} \frac{\partial V_{j\nu}}{\partial p_{i\mu}}, \quad \frac{dp_i^\mu}{dt} = \sum_j v_j^{*\nu} \frac{\partial V_{j\nu}}{\partial q_{i\mu}}, \tag{4}$$

where $v_i^{*\mu} = p_i^{*\mu}/p_i^{*0}$. For the momentum-dependent part, we replace $(\boldsymbol{p}_i - \boldsymbol{p}_j)^2$ in Eq. (3) with the two-body relative momentum squared, $p_{R,ij}^2$, in the rest frame of the particle j. We use U_Λ^μ in Eq. (1) for Λ and other hyperons.[1]

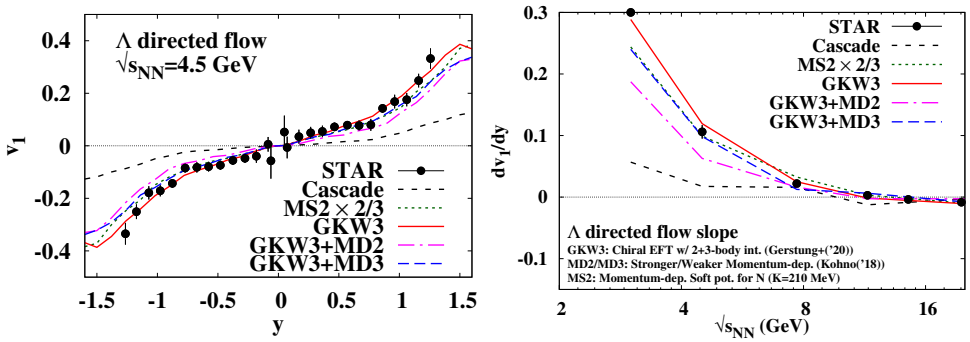

Figure 2. Left: Calculated directed flow of Λ in mid-central Au + Au collisions at $\sqrt{s_{NN}}$ = 4.5 GeV. Right: The directed flow slope of Λ. Data are taken from Ref. [7].

In Fig. 2, we compare the calculated Λ directed flow $v_1 = \langle \cos\phi \rangle$ in the impact parameter range 4.6 fm $< b <$ 9.4 fm with the STAR data [7] in midcentral Au + Au collisions at $\sqrt{s_{NN}}$ = 4.5 GeV (left panel), and the directed flow slope of Λ at $\sqrt{s_{NN}}$ = (3.0-19.6) GeV (right panel). The cascade results (without potential effects) underestimate the data. With the potential effects, the directed flow data of Λ are roughly explained. Specifically, GKW3 without momentum dependence explains the data well.[2]

[1] In the HYP2022 presentation, I answered to the question by Hoai Le that we do include different potentials for Σ and Ξ, but it was not correct. The results shown in HYP2022 and in this proceedings are obtained by assuming the same potential for all hyperons.

[2] In the HYP2022 presentation, we showed the calculated results with an incorrect p_T cut at $\sqrt{s_{NN}}$ = 3.0 GeV, and the GKW3 results underestimated the directed flow data. By using the correct cut adopted in the experimental data analysis, 0.4 GeV $\leq p_T \leq$ 2.0 GeV [7], the results from GKW3 explain the directed flow well also at $\sqrt{s_{NN}}$ = 3.0 GeV.

Now let us discuss the sensitivity of the directed flow to the density- and momentum-dependence of the Λ potential. Unfortunately, GKW2, not shown in the figure, gives the Λ directed flow similar to that from GKW3. Thus we cannot discriminate the Λ potentials from χEFT with 2- and 2+3-body interactions by the directed flow. We also note that the strong momentum dependence of the Λ potential, e.g. GKW3+MD2, reduces the directed flow, especially at large rapidities [12]. We do not completely understand the origin of this dependence, but we guess that the cancellation of the contributions in the compression and expansion stages is one of the origins. The repulsive potential at high densities increases the directed flow in the compression stage, but a part of the increase is canceled by the negative contribution from the expansion of the tilted matter.

4 Summary and discussion

We have investigated the Λ potential via the Λ directed flow from heavy-ion collisions [12]. We implement the Λ potential from the χEFT [3, 4] parameterized as a function of density and momentum in the RQMDv mode of an event generator JAM. The calculated results using the Λ potential from χEFT do reproduce the Λ directed flow in a wide beam energy range. This is the first support by experimental data of the strongly repulsive Λ potential at high densities. It should be noted that similar results are obtained for the sideward flow $\langle p_x \rangle$ at $\sqrt{s_{NN}} = 2.7$ GeV in Ref. [21].

Yet there are several questions and problems. First, the directed flow of Λ can also be reproduced by the Λ potential only from the 2-body interactions and with a weaker repulsion at high densities. Next, the Λ directed flow depends on the momentum dependence of the potential, especially at large rapidities. Provided that the compression/expansion mechanism [10] is correct, the directed flow of Λs produced during the compression stage is affected by the expansion of tilted matter and would be more sensitive to dependence on momentum than density. More analyses of the evolution are needed to understand the sensitivity to the details of the Λ potential.

It is interesting to study Ξ and Σ flows as well. These are related to the repulsive Σ potential in dense matter [21], the dense matter EoS [22], and the formation of deconfined matter [23].

The authors would like to thank Yue-Hang Leung for telling us that the p_T cut is different at $\sqrt{s_{NN}} = 3.0$ GeV. This work was supported in part by the Grants-in-Aid for Scientific Research from JSPS (No. JP21K03577, No. JP19H01898, and No. JP21H00121).

References

[1] P. Demorest *et al.*, Nature **467**, 1081 (2010); E. Fonseca *et al.*, Astrophys. J. **832**, 167 (2016); J. Antoniadis *et al.*, Science **340**, 6131 (2013); H. T. Cromartie *et al.* [NANOGrav], Nature Astron. **4**, 72 (2019); M. C. Miller *et al.*, Astrophys. J. Lett. **918**, L28 (2021)

[2] S. Nishizaki, T. Takatsuka and Y. Yamamoto, Prog. Theor. Phys. **108**, 703 (2002); J. Rikovska-Stone, P. A. M. Guichon, H. H. Matevosyan and A. W. Thomas, Nucl. Phys. A **792**, 341 (2007); S. Weissenborn, D. Chatterjee and J. Schaffner-Bielich, Phys. Rev. C **85**, 065802 (2012) [erratum: Phys. Rev. C **90**, 019904 (2014)]; T. Miyatsu, S. Yamamuro and K. Nakazato, Astrophys. J. **777**, 4 (2013). H. Togashi, E. Hiyama, Y. Yamamoto and M. Takano, Phys. Rev. C **93**, 035808 (2016)

[3] D. Gerstung, N. Kaiser, W. Weise, Eur. Phys. J. A **56**, 175 (2020)

[4] M. Kohno, Phys. Rev. C **97**, 035206 (2018)

[5] S. Petschauer, J. Haidenbauer, N. Kaiser, U. G. Meißner and W. Weise, Nucl. Phys. A **957**, 347 (2017); J. Haidenbauer, S. Petschauer, N. Kaiser, U. G. Meißner and W. Weise, Eur. Phys. J. C **77**, 760 (2017)

[6] K. Aoki *et al.*, *Extension of the J-PARC Hadron Experimental Facility: Third White Paper*, arXiv:2110.04462 [nucl-ex]

[7] L. Adamczyk *et al.* [STAR], Phys. Rev. Lett. **112**, 162301 (2014); P. Shanmuganathan *et al.* [STAR], Nucl. Phys. A **956**, 260 (2016); L. Adamczyk *et al.* [STAR], Phys. Rev. Lett. **120**, 062301 (2018); J. Adam *et al.* [STAR], Phys. Rev. C **103**, 034908 (2021); M. S. Abdallah *et al.* [STAR], Phys. Lett. B **827**, 137003 (2022)

[8] J. Steinheimer, J. Auvinen, H. Petersen, M. Bleicher and H. Stoecker, Phys. Rev. C **89**, 054913 (2014); Y. B. Ivanov and A. A. Soldatov, Phys. Rev. C **91**, 024915 (2015); Y. B. Ivanov and A. A. Soldatov, Eur. Phys. J. A **52**, 10 (2016); Y. Nara, H. Niemi, J. Steinheimer and H. Stoecker. Phys. Lett. B **769**, 543 (2017)

[9] V. P. Konchakovski, W. Cassing, Y. B. Ivanov and V. D. Toneev, Phys. Rev. C **90**, 014903 (2014)

[10] Y. Nara and A. Ohnishi, Phys. Rev. C **105**, 014911 (2022)

[11] Y. Nara, N. Otuka, A. Ohnishi, K. Niita and S. Chiba, Phys. Rev. C **61**, 024901 (2000)

[12] Y. Nara, A. Jinno, K. Murase and A. Ohnishi, Phys. Rev. C **106**, 044902 (2022) [arXiv:2208.01297 [nucl-th]]

[13] S. Balberg and A. Gal, Nucl. Phys. A **625**, 435 (1997); D. E. Lanskoy and Y. Yamamoto, Phys. Rev. C **55**, 2330 (1997); M. Baldo, G. F. Burgio and H. J. Schulze, Phys. Rev. C **61**, 055801 (2000)

[14] N. K. Glendenning and S. A. Moszkowski, Phys. Rev. Lett. **67**, 2414 (1991); J. Schaffner and I. N. Mishustin, Phys. Rev. C **53**, 1416 (1996); C. Ishizuka, A. Ohnishi, K. Tsubakihara, K. Sumiyoshi and S. Yamada, J. Phys. G **35**, 085201 (2008); H. Shen, H. Toki, K. Oyamatsu and K. Sumiyoshi, Astrophys. J. Suppl. **197**, 20 (2011)

[15] P. Danielewicz, P. B. Gossiaux and R. A. Lacey, Fundam. Theor. Phys. **95**, 69 (1999); A. Sorensen and V. Koch, Phys. Rev. C **104**, 034904 (2021); C. Fuchs and H. H. Wolter, Nucl. Phys. A **589**, 732 (1995); K. Weber, B. Blaettel, W. Cassing, H. C. Doenges, V. Koch, A. Lang and U. Mosel, Nucl. Phys. A **539**, 713 (1992)

[16] Y. Fujiwara, Y. Suzuki and C. Nakamoto, Prog. Part. Nucl. Phys. **58**, 439 (2007)

[17] JAM2, an event generator for high-energy nuclear collisions, https://gitlab.com/transportmodel/jam2

[18] T. Sjöstrand, S. Ask, J. R. Christiansen, R. Corke, N. Desai, P. Ilten, S. Mrenna, S. Prestel, C. O. Rasmussen and P. Z. Skands, Comput. Phys. Commun. **191**, 159-177 (2015), https://pythia.org/

[19] X. L. Zhao, G. L. Ma, Y. G. Ma and Z. W. Lin, Phys. Rev. C **102**, 024904 (2020)

[20] H. Sorge, Phys. Rev. C **52**, 3291 (1995); Y. Nara and H. Stoecker, Phys. Rev. C **100**, 054902 (2019); Y. Nara, T. Maruyama and H. Stoecker, Phys. Rev. C **102**, 024913 (2020)

[21] D. C. Zhang, H. G. Cheng and Z. Q. Feng, Chin. Phys. Lett. **38**, 092501 (2021)

[22] G. C. Yong, Z. G. Xiao, Y. Gao and Z. W. Lin, Phys. Lett. B **820**, 136521 (2021)

[23] K. Nayak, S. Shi, N. Xu and Z. W. Lin, Phys. Rev. C **100**, 054903 (2019)